A Triangular Copper(I) Complex Displaying Allosteric Cooperativity in Its Electrochemical Behavior and a Mixed-Valence Cu(I)−Cu(I)−Cu(II) State with Unusual Temperature-Dependent Behavior

Peter L. Jones,[†] John C. Jeffery,[†] John P. Maher,[†] Jon A. McCleverty,*[,†] Philip H. Rieger,[‡] and Michael D. Ward*[,†]

School of Chemistry, University of Bristol, Cantock's Close, Bristol BS8 1TS, U.K., and Department of Chemistry, Brown University, Providence, Rhode Island 02912

Received January 24, 1997[⊗]

Reaction of the tris-chelating hexadentate podand ligand tris[3-(2-pyridyl)pyrazol-1-yl]hydroborate (Tp^{Py}) with $[Cu(MeCN)_4][PF_6]$ affords $[Cu^I_3(Tp^{Py})_2][PF_6]$ (**1**), which was crystallographically characterized. **1**·$(MeCN)_2$: $C_{52}H_{44}B_2Cu_3F_6N_{20}P$, orthorhombic, *Pna*$2_1$; $a = 24.592(7)$, $b = 16.392(5)$, $c = 13.365(5)$ Å; $Z = 4$. Each Cu(I) ion is four coordinated by one *N,N′*-bidentate arm from each ligand; each ligand therefore donates each bidentate arm to a different Cu(I) ion. The isosceles triangular arrangement of Cu(I) ions with N-donor ligands is reminiscent of the tricopper(I) site of ascorbate oxidase. One-electron oxidation of **1** affords the $Cu^I_2Cu^{II}$ complex $[Cu_3(Tp^{Py})_2][PF_6]_2$ (**2**). The potentials of the Cu(I)/Cu(II) redox couples are affected by the ease with which the accompanying geometric rearrangement can occur. Thus, the first oxidation of **1** is facile (−0.52 V *vs* the ferrocene/ferrocenium couple, Fc/Fc^+), but as a result of the concomitant structural rearrangement the second oxidation is rendered much more difficult (+0.12 V *vs* Fc/Fc^+) and results in slow decomposition of the product. A third oxidation does not occur at accessible potentials. This complex therefore exhibits negative cooperative behavior, in which the geometric change accompanying one metal-based redox change hinders further redox changes at other sites *via* an allosteric effect. EPR studies on the mixed-valence complex **2** show that in frozen glasses below 120 K the unpaired electron is delocalized over *two* metal centers (7-line spectrum), but above 160 K the electron becomes localized and gives a simple axial spectrum. The electronic spectrum of **2** in solution shows an intense band at 910 nm (ϵ 2100 $dm^3\ mol^{-1}\ cm^{-1}$) which we believe to be an IVCT band. The combination of EPR and electronic spectral studies show that **2** is class III (fully delocalized over 2 centers) below 120 K but class II (localized but strongly interacting) at higher temperatures.

Copper(I) complexes are of interest in coordination chemistry for many reasons. Simple mononuclear complexes of N-heterocyclic ligands (particularly derivatives of 2,2′-bipyridine and 1,10-phenanthroline) have been popular targets of study because of their photophysical, electrochemical, structural, and spectroscopic properties.[1−4] Polynuclear copper centers are widespread in biological systems, occurring, for example, in the type 3 cuproproteins, such as tyrosinase and hemocyanin, and the multinuclear oxidases, such as ascorbate oxidase, laccase, and nitrous oxide reductase,[5] all of which can exist in fully reduced Cu(I) states and have been extensively modeled.[6] Oxidation of one of the copper centers in a polynuclear species can afford mixed-valence Cu(I)/Cu(II) complexes.[7] These are of particular interest in the rare cases when the mixed-valence state is delocalized,[8,9] as well as being of particular relevance to modeling the behavior of metalloproteins such as nitrous oxide reductase in which a mixed-valence state is known to be involved in the catalytic cycle.[10]

We describe here the synthesis, crystal structure, and electrochemical and spectroscopic properties of the trinuclear copper(I) complex $[Cu_3(Tp^{Py})_2][PF_6]$ (**1**) (Tp^{Py} is the hexadentate podand ligand tris[3-(2-pyridyl)pyrazol-1-yl]hydroborate)[11−15] and also the synthesis and properties of its one-electron oxidation

[†] University of Bristol.
[‡] Brown University.
[⊗] Abstract published in *Advance ACS Abstracts,* June 1, 1997.

(1) (a) Bardwell, D. A.; Cargill Thompson, A. M. W.; Jeffery, J. C.; Tilley, E. E. M.; Ward, M. D. *J. Chem. Soc., Dalton Trans.* **1995**, 835 and references therein. (b) Bardwell, D. A.; Jeffery, J. C.; Otter, C. A.; Ward, M. D. *Polyhedron* **1996**, *15*, 191. (c) McMaster, J.; Beddoes, R. L.; Collison, D.; Eardley, D. R.; Helliwell, M.; Garner, C. D. *Chem. Eur. J.* **1996**, *2*, 685. (d) Comba, P.; Hambley, T. W.; Hilfenhaus, P.; Richens, D. T. *J. Chem. Soc., Dalton Trans.* **1996**, 533.
(2) Federlin, P.; Kern, J.-M.; Rastegar, A.; Dietrich-Buchecker, C.; Marnot, P. A.; Sauvage, J.-P. *New J. Chem.* **1990**, *14*, 9.
(3) Dobson, J. F.; Green, B. E.; Healy, P. C.; Kennard, C. H. L.; Pakawatchai, C.; White, A. H. *Aust. J. Chem.* **1984**, *37*, 649.
(4) Horváth, O.; Stevenson, K. L. *Charge Transfer Photochemistry of Coordination Compounds*; VCH: New York, 1993.
(5) Kaim, W.; Schwederski, B. *Bioinorganic Chemistry: Inorganic Elements in the Chemistry of Life*; Wiley: Chichester, U.K., 1995.
(6) (a) Kitajima, N.; Moro-oka, Y. *Chem. Rev.* **1994**, *94*, 737. (b) Sorrell, T. N. *Tetrahedron* **1989**, *45*, 3. (c) Kitajima, N.; Moro-oka, Y. *J. Chem. Soc., Dalton Trans.* **1993**, 2665. (d) Lee, D.-H.; Wei, N.; Murthy, N. N.; Tyeklár, Z.; Karlin, K. D.; Kaderli, S.; Jung, B.; Zuberbühler, A. D. *J. Am. Chem. Soc.* **1995**, *117*, 12498 and references therein.
(7) Dunaj-Jurco, M.; Ondrejovic, G.; Melník, M. *Coord. Chem. Rev.* **1988**, *83*, 1.
(8) (a) Harding, C.; McKee, V.; Nelson, J.; *J. Am. Chem. Soc.* **1991**, *113*, 9684. (b) Barr, M. E.; Smith, P. H.; Antholine, W. E.; Spencer, B. *J. Chem. Soc., Chem. Commun.* **1993**, 1649. (c) Harding, C.; Nelson, J.; Symons, M. C. R.; Wyatt, J. *J. Chem. Soc., Chem. Commun.* **1994**, 2499.
(9) (a) Sigwart, C.; Hemmerich, P.; Spence, J. T. *Inorg. Chem.* **1968**, *7*, 2545. (b) Gatteschi, D.; Mealli, C.; Sacconi, L. *Inorg. Chem.* **1976**, *15*, 2774. (c) Gagné, R. R.; Koval, C. A.; Smith, T. J.; Cimolino, M. C. *J. Am. Chem. Soc.* **1979**, *101*, 4571. (d) Long, R. C.; Hendrickson, D. N.; *J. Am. Chem. Soc.* **1983**, *105*, 1513.
(10) (a) Houser, R. P.; Young, V. G., Jr.; Tolman, W. B. *J. Am. Chem. Soc.* **1996**, *118*, 2101. (b) Halfen, J. A.; Mahapatra, S.; Wilkinson, E. C.; Gengenbach, A. J.; Young, V. G., Jr.; Que, L., Jr.; Tolman, W. B. *J. Am. Chem. Soc.* **1996**, *118*, 763. (c) Houser, R. P.; Tolman, W. B. *Inorg. Chem.* **1995**, *34*, 1632. (d) Neese, F.; Zumft, W. G.; Antholine, W. E.; Kroneck, P. M. H. *J. Am. Chem. Soc.* **1996**, *118*, 8692. (e) Westmoreland, T. D.; Wilcox, D. E.; Baldwin, M. J.; Mims, W. B.; Solomon, E. I. *J. Am. Chem. Soc.* **1989**, *111*, 6106.
(11) Jones, P. L.; Amoroso, A. J.; Jeffery, J. C.; McCleverty, J. A.; Psillakis, E.; Rees, L. H.; Ward, M. D. *Inorg. Chem.* **1997**, *36*, 10.

S0020-1669(97)00088-8 CCC: $14.00

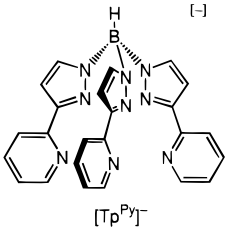

$[Tp^{Py}]^-$

mixed-valence Cu(I)/Cu(I)/Cu(II) product $[Cu_3(Tp^{Py})_2][PF_6]_2$ (**2**). These complexes have many unusual features. First, synthesis of **1** is a good example of a multicomponent self-assembly reaction in which the nature of the product is dictated by the complementarity between the geometric preferences of the metal ion and the number, type, and geometric arrangement of the coordination sites provided by the ligands. Second, the approximately isosceles triangular arrangement of metal atoms in these complexes, and the N-donor ligand set, make them a good structural model for the trinuclear copper site of the multicopper oxidases such as ascorbate oxidase and laccase. Third, the rigidity of the ligand framework results in interesting electrochemical properties, in particular a separation between two Cu(I)/Cu(II) couples at (initially) chemically equivalent sites which is much larger than be accounted for by electronic interactions, and which points to allosteric effects controlling redox potentials. Fourth, the mixed-valence complex **2** shows unusual temperature-dependent EPR properties which are characteristic of two-center delocalization at low temperatures but localization at higher temperatures.

Experimental Section

General Methods. ^{1}H NMR spectra were recorded on Jeol GX270, Lambda 300, or GX400 spectrometers. UV/vis spectra were obtained at room temparature on a Perkin-Elmer Lambda 19 instrument. Fast atom bombardment (FAB) mass spectra were recorded on a VG Autospec instrument, with 3-nitrobenzyl alcohol as matrix. Electrospray mass spectra were performed with MeCN solutions of the complexes on a VG Quattro instrument, using cone voltages of typically 25 V. Electrochemical measurements were made with a PC-controlled EG&G/PAR 273A potentiostat, using platinum bead working and auxiliary electrodes, and an SCE reference electrode. The measurements were performed using acetonitrile distilled over calcium hydride, with 0.1 mol dm^{-3} $[NBu^n_4][PF_6]$ as supporting electrolyte. Ferrocene was added at the end of each experiment as an internal reference, and all redox potentials are quoted *vs* the ferrocene/ferrocenium couple (Fc/Fc^+). EPR spectra of **2** were recorded in a 1,2-dichloroethane/thf (1:1) solvent mixture over the range 77−355 K, using a Bruker ESP-300E spectrometer equipped with a Bruker ER 4121VT-RS variable-temperature unit and a Eurotherm temperature controller. The sample concentrations were typically 10^{-3} M; no variation in the spectra with concentration were observed at this degree of dilution. The microwave power was 20 mW and the modulation amplitude 1−2 G.

$K[Tp^{Py}]$[11] and $[Cu(MeCN)_4][PF_6]$[16] were prepared according to the published methods. Reagents were obtained from Aldrich, Lancaster, or Avocado and used as received.

Preparations. Complex 1. A mixture of $[Cu(MeCN)_4][PF_6]$ (0.28 g, 0.75 mmol) and $K(Tp^{Py})$ (0.24 g, 0.50 mmol) in dry MeCN (40 cm^3) under N_2 was stirred for 2 h to give a red-brown solution. After concentration *in vacuo*, addition of dry MeOH (20 cm^3) to the residue resulted in precipitation of a brown solid and left a green solution. The solid was filtered off under N_2, washed with a further portion of MeOH, and dried to give **1** (0.15 g, 50%). ES-MS [*m/z* (relative intensity, assignment]: 1223 (5%, **1**), 1079 (90%, **1** − PF_6), 507 (100%, $\{Cu(Tp^{Py})\}$). Anal. Found: C, 47.3; H, 3.4; N, 20.3. Calcd for $C_{48}H_{38}N_{18}B_2Cu_3P_2F_{12}$: C, 47.1; H, 3.1; N, 20.6%. UV/vis spectrum [MeCN; λ_{max}/nm ($10^{-3}\epsilon$, dm^3 mol^{-1} cm^{-1})]: 258 (57), 286 (41), 314 (sh), 390 (5.4).

Complex 2. The green filtrate left from synthesis of **1** was evaporated to dryness. The resulting green solid was dissolved in CH_2Cl_2 and filtered to remove KPF_6; the solution was then evaporated to dryness, and the product was recrystallized from MeCN/ether to give **2** (0.14 g, 41%). Alternatively, **1** (10 mg, 8.2 μmol) was treated with $[Cp_2Fe][PF_6]$ (2.7 mg, 8.2 μmol) in CH_2Cl_2 or MeCN solution. After evaporation to dryness the ferrocene was removed by prolonged warming *in vacuo* and the product recrystallized as before. ES-MS [*m/z* (relative intensity, assignment]: 1079 (20%, **2** − 2PF_6), 507 (100%, $\{Cu(Tp^{Py})\}$). Anal. Found: C, 42.7; H, 2.5; N, 18.0. Calcd for $C_{48}H_{38}N_{18}B_2Cu_3PF_6$: C, 42.1; H, 2.8; N, 18.4%. UV/vis spectrum [MeCN; λ_{max}/nm ($10^{-3}\epsilon$, dm^3 mol^{-1} cm^{-1})]: 247 (55), 287 (39), 370 (3.4), 450 (sh), 910 (2.1).

X-ray Crystallography. X-ray-quality crystals of **1**·$(MeCN)_2$ were grown by slow evaporation from MeCN. A suitable brown block (0.35 × 0.3 × 0.1 mm^3) was rapidly transferred from the mother liquor to a cold stream of N_2 (−105 °C) on a Siemens SMART three-circle diffractometer fitted with a CCD-type area detector. Graphite-monochromatized Mo K_α X-radiation ($\bar{\lambda}$ = 0.710 73 Å) was used. Crystal data are summarized in Table 1. A total of 14 685 data were collected at −105 °C with $4.5 \le 2\theta \le 46.5°$. Data were collected for Lorentz−polarization effects and for absorption effects by an empirical method based on multiple measurements of equivalent data. After the merging of data, these gave 5664 independent reflections (R_{int} = 0.0555). The structure was solved by conventional direct methods and was refined by the full-matrix least-squares method on all F^2 data with the SHELXTL 5.03 package[17] using a Silicon Graphics Indy computer. All non-hydrogen atoms were refined anisotropically; hydrogen atoms were included in calculated positions and refined with isotropic thermal parameters. Refinement of 760 parameters converged at R_1 (selected data) = 0.056; wR_2 (all data) = 0.137. The largest residual peak and hole were +0.85 and −0.58 e Å^{-3}. Selected bond lengths and angles are in Table 2.

Table 1. Crystallographic Data for **1**·2MeCN

empirical formula	$C_{52}H_{44}B_2Cu_3F_6N_{20}P$
fw	1306.28
space group	$Pna2_1$
a, Å	24.592(7)
b, Å	16.392(5)
c, Å	13.365(5)
V, Å^3	5387(3)
Z	4
ρ_{calc}, g cm^{-3}	1.611
μ, mm^{-1}	1.284
T, K	173(2)
λ, Å	0.710 73
R_1, wR_2[a]	0.056, 0.137

[a] Structure was refined on F_o^2 using all data: $wR_2 = [\sum[w(F_o^2 - F_c^2)^2]/\sum w(F_o^2)^2]^{1/2}$, where $w^{-1} = [\sigma^2(F_o^2) + (0.0492P)^2 + 25.78P]$ and $P = [\max(F_o^2,0) + 2F_c^2]/3$. The value in parentheses for R_1 is given for comparison with older refinements based on F_o with a typical threshold of $F \ge 4\sigma(F)$ and $R_1 = \sum||F_o| - |F_c||/\sum|F_o|$ and $w^{-1} = [\sigma^2(F_o) + gF_o^2]$.

Results and Discussion

Synthesis and Crystal Structure of 1. The podand ligand $[Tp^{Py}]^-$ on which these complexes are based can form polynuclear complexes with first-row transition-metal ions by

(12) Amoroso, A. J.; Jeffery, J. C.; Jones, P. L.; McCleverty, J. A.; Thornton, P.; Ward, M. D. *Angew. Chem., Int. Ed. Engl.* **1995**, *34*, 1443.
(13) Amoroso, A. J.; Jeffery, J. C.; Jones, P. L.; McCleverty, J. A.; Psillakis, E.; Ward, M. D. *J. Chem. Soc., Chem. Commun.* **1995**, 1175.
(14) (a) Amoroso, A. J.; Jeffery, J. C.; Jones, P. L.; McCleverty, J. A.; Rees, L.; Rheingold, A. L.; Sun, Y.; Takats, J.; Trofimenko, S.; Ward, M. D.; Yapp, G. P. A. *J. Chem. Soc., Chem. Commun.* **1995**, 1881. (b) Amoroso, A. J.; Jeffery, J. C.; Jones, P. L.; McCleverty, J. A.; Ward, M. D. *Polyhedron* **1996**, *15*, 2023.
(15) Bardwell, D. A.; Jeffery, J. C.; Jones, P. L.; McCleverty, J. A.; Ward, M. D. *J. Chem. Soc., Dalton Trans.* **1995**, 2921.
(16) Kubas, G. J. *Inorg. Synth.* **1976**, *19*, 90.
(17) SHELXTL 5.03 program system; Siemens Analytical X-Ray Instruments, Madison, WI, 1995.

Table 2. Selected Bond Lengths (Å) and Angles (deg) for **1**·2MeCN

Cu(1)−N(212)	1.932(7)	Cu(2)−N(132)	1.968(9)	Cu(3)−N(232)	1.936(9)
Cu(1)−N(112)	1.965(7)	Cu(2)−N(252)	1.965(9)	Cu(3)−N(152)	1.966(8)
Cu(1)−N(122)	2.117(8)	Cu(2)−N(262)	2.186(9)	Cu(3)−N(162)	2.193(8)
Cu(1)−N(222)	2.143(7)	Cu(2)−N(142)	2.209(7)	Cu(3)−N(242)	2.262(7)
N(212)−Cu(1)−N(112)	156.2(3)	N(132)−Cu(2)−N(252)	163.0(3)	N(232)−Cu(3)−N(152)	165.8(3)
N(212)−Cu(1)−N(122)	114.1(3)	N(132)−Cu(2)−N(262)	117.5(3)	N(232)−Cu(3)−N(162)	114.0(3)
N(112)−Cu(1)−N(122)	81.5(3)	N(252)−Cu(2)−N(262)	79.4(3)	N(152)−Cu(3)−N(162)	79.8(3)
N(212)−Cu(1)−N(222)	81.7(3)	N(132)−Cu(2)−N(142)	80.1(3)	N(232)−Cu(3)−N(242)	79.8(3)
N(112)−Cu(1)−N(222)	111.0(3)	N(252)−Cu(2)−N(142)	100.2(3)	N(152)−Cu(3)−N(242)	96.5(3)
N(122)−Cu(1)−N(222)	109.4(2)	N(262)−Cu(2)−N(142)	100.7(3)	N(162)−Cu(3)−N(242)	94.1(3)
N(111)−B(1)−N(151)	111.4(8)	N(111)−B(1)−N(131)	112.7(9)	N(151)−B(1)−N(131)	110.8(8)
N(211)−B(2)−N(251)	112.2(8)	N(211)−B(2)−N(231)	114.4(8)	N(251)−B(2)−N(231)	112.8(8)

utilizing a binding mode in which each bidentate arm coordinates to a different metal ion.[12,13] This occurs because the ligand cavity is too large for such small ions, so a coordination mode in which the metal ion sites within the ligand cavity, coordinated by all three bidentate arms, is not possible. This is in direct contrast to the structures that form with lanthanides, actinides, and the heavier main-group metal ions, where "inclusion" complexes are the norm.[11,13,14]

The propensity of Cu(I) to form four-coordinate pseudotetrahedral complexes with diimines[1−3] suggested that a 3:2 metal:ligand stoichiometry would be needed, both to give each metal ion its preferred pseudotetrahedral four-coordinate environment and to use all of the ligand binding sites. Reaction of $K(Tp^{Py})$ with $[Cu(MeCN)_4][PF_6]$ in MeCN afforded a brown complex whose elemental analysis and mass spectrum were in agreement with this, suggesting the formulation $[Cu_3(Tp^{Py})_2][PF_6]$ (**1**). This contrasts with the tetramers $[M_4(Tp^{Py})_4][PF_6]_4$ that form with dications such as Mn(II) which prefer six-coordinate tris-chelate coordination. This reaction also afforded a second, partially oxidized, material whose mass spectrum also showed a 3:2 Cu:Tp^{Py} stoichiometry but whose elemental analysis indicated the formulation to be $[Cu_3(Tp^{Py})_2][PF_6]_2$, i.e. a $Cu^I_2Cu^{II}$ complex (**2**) formed by partial oxidation of **1**.

Given the steric inability of $[Tp^{Py}]^-$ to confer tetrahedral geometry on a metal ion—it is not possible for two of its arms to be mutually perpendicular and still coordinate to the same metal—we thought that the most likely structure for **1** was that each metal ion would be coordinated by a different arm from each of the two ligands, as for the Ag(I) analogue $[Ag_3(Tp^{Py})_2][ClO_4]$.[13] The crystal structure of **1**·$(MeCN)_2$ (Figure 1) confirmed this. Each Cu(I) ion is in a distorted four-coordinate geometry arising from coordination by one bidentate arm from each ligand, with the two ligands "capping" the Cu_3 core. The metal ions are crystallographically independent: the Cu(1)−Cu(2), Cu(2)−Cu(3), and Cu(1)−Cu(3) separations are 3.614, 2.915 and 3.500 Å respectively. The geometries about the metals are sufficiently distorted for the description "pseudotetrahedral" to be inappropriate. Figure 2a shows a simplified view of the structure with just the metal ions, the nitrogen donor atoms, and the metal−metal separations. Most of the Cu−N bond lengths lie in the typical range for Cu(I) complexes,[1−3] but the bonds to Cu(2) and Cu(3) of their pyridyl donors are rather long (2.19−2.26 Å). The N−B−N angles lie in the range 110.8−114.4°, somewhat greater than the ideal tetrahedral angles which occur when the ligand coordinates in a strain-free manner, suggesting that the ligand arms are slightly "splayed out" to accommodate three Cu(I) ions within the cavity of each ligand. The dihedral angles θ between the two CuN_2 planes are 80.7, 84.4, and 88.6° at Cu(1), Cu(2), and Cu(3) respectively.

There are π-stacking interactions between overlapping sections of the aromatic ligands. In particular, since the Cu(2)···Cu(3) separation is the shortest of the three Cu···Cu separations, pyridyl rings C(261)−C(266) and C(161)−C(166) are involved in the most obvious $\pi-\pi$ interaction with the distances of the atoms in one ring from the mean plane of the other lying in the range 3.2−3.6 Å. The overlapping segments are not exactly "face-to-face" but "slipped" relative to one another.

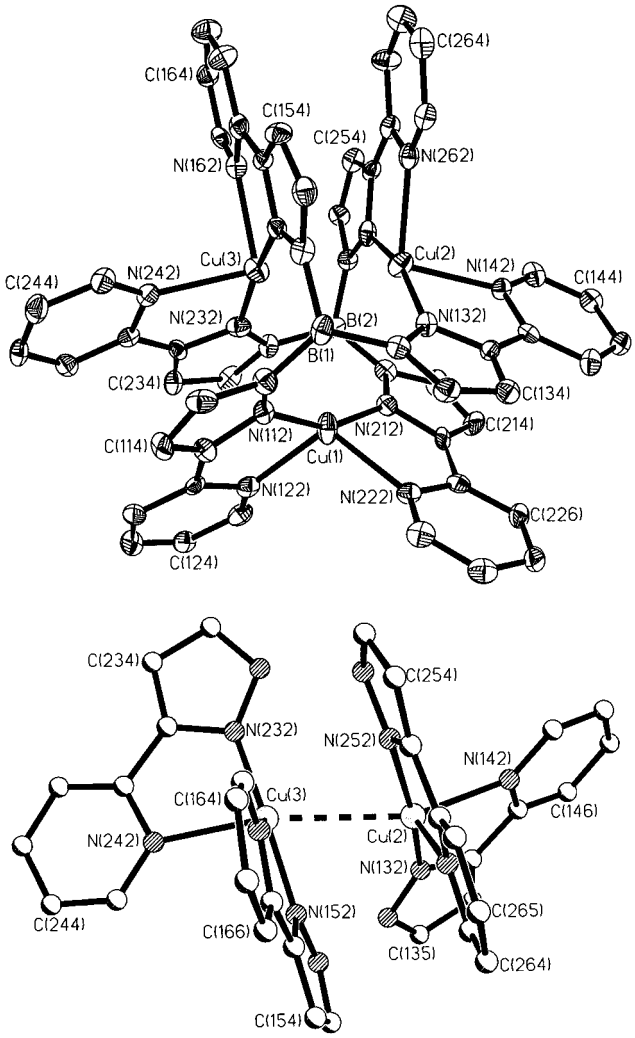

Figure 1. (a) Top: Structure of the complex cation of **1**, $[Cu_3(Tp^{Py})_2]^+$, showing 35% thermal ellipsoids. (b) Bottom: View of atoms Cu(2) and Cu(3) and their associated ligands, emphasizing the π-stacking of aromatic ligands attached to them.

The two longer metal−metal separations are too large for there to be any direct metal−metal bonding interactions. The shortest Cu−Cu separation (2.915 Å) possibly represents a weak bonding interaction, although it is comparable to that observed in the cubane $[(Et_3P)CuI]_4$ (2.93 Å) in which it was also assumed that there was no direct metal−metal interaction,[18] and is rather larger than the Cu−Cu distances which commonly indicate a

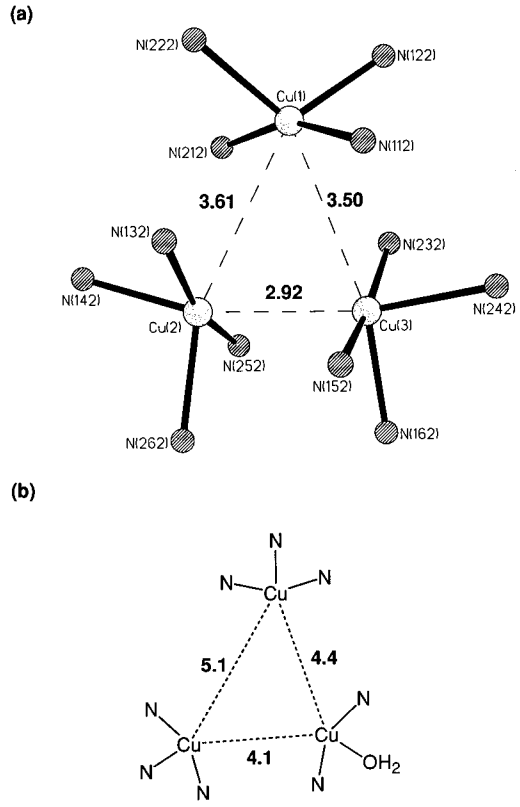

Figure 2. Simplified views of (a) **1**, showing just the metal ions and the coordinated N atoms, and (b) the tricopper(I) site of ascorbate oxidase. Metal−metal separations are in Å.

definite bonding interaction (*ca.* 2.4−2.7 Å).[19] It is also considerably longer than the Cu−Cu distance in metallic copper (2.56 Å). The asymmetry which is apparent in the solid state is however not present in solution. The ^{1}H NMR spectrum of **1** in DMSO-d^6, although being slightly broadened due to oxidation (even in the presence of ascorbic acid), clearly showed the presence of 6 aromatic proton environments, indicating a 3-fold-symmetric structure in solution with all three metal sites equivalent and both ligands equivalent. If we assume that the Cu−Cu distances in solution are approximately the average of those in the solid state, they will be around 3.3 Å, too large for a direct Cu−Cu bonding interaction, so **1** may be considered to contain three distinct $\{Cu(NN)_2\}^+$ fragments linked by the apical boron atoms of the podand ligands.

The crystal structure of **1** is of particular interest for two reasons. First, triangular copper(I) complexes of any sort are relatively rare.[20−22] Most of those that are known are based on μ^2 P-donor or S-donor fragments from edge-bridging ligands

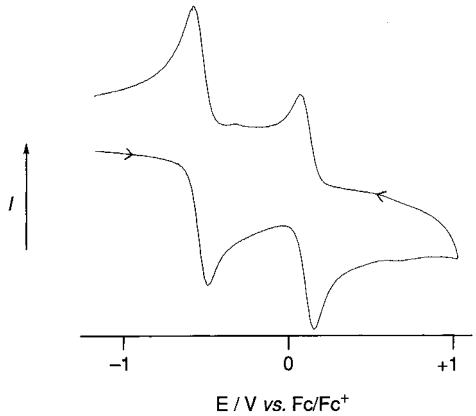

Figure 3. Cyclic voltammogram of **1** in MeCN at a Pt-bead working electrode at a scan rate of 1 V s^{-1}.

such as ethane-1,2-dithiolate or bis(diphenylphosphino)methane:[21] complexes with N-donor ligand sets are particularly scarce.[22] The second point of interest lies in the recent discovery that multicopper oxidases such as ascorbate oxidase contain an approximately isosceles triangle of copper atoms, which comprises a mononuclear type 2 copper center in close proximity to a dinuclear type 3 copper center.[5,23] The structural properties of the tricopper site of ascorbate oxidase in its fully reduced form is shown in Figure 2b, together with the principal structural parameters for the tricopper core of **1** (Figure 2a). Structural models for this tricopper unit are rare,[22,24] particularly in the fully reduced form. The metal−metal separations in **1** are significantly shorter than those in ascorbate oxidase, but both the geometry of the metal triangle and the N-donor ligand environment around each metal ion are reminiscent of the enzyme active site. The metal−metal separations in **1** actually correspond more closely to those in the fully oxidized form of the ascorbate oxidase active site in which the Cu(II)···Cu(II) separations shorten to the range 3.4−4.0 Å. We note that pyrazolyl ligands [generally from tris(pyrazolyl)borates] have been widely used as reasonable mimics of imidazole ligation in metalloprotein model complexes.[6,25]

Electrochemical Studies. Cyclic and square-wave voltammetry on **1** in MeCN showed two redox processes at $E_{1/2}$ = −0.52 and +0.12 V *vs* the ferrocene/ferrocenium couple (Fc/Fc$^+$), which are metal-based Cu(I)/Cu(II) couples (Figure 3). The first redox couple is fully chemically reversible at all scan rates (cathodic and anodic peak currents equal; peak−peak separation 70 mV and virtually invariant with scan rate), which is consistent with the fact that the one-electron oxidation product **2** could be isolated and is indefinitely stable. The second is chemically reversible at high scan rates (cf. Figure 3, which was recorded at 1 V s^{-1}), but the return wave diminishes in intensity as the scan rate decreases and at a scan rate of 0.1 V s^{-1} is only about half the intensity of the outward wave. This is consistent with slow decomposition of the doubly oxidized $Cu^ICu^{II}_2$ species. A third oxidation is not apparent within the

(18) (a) Churchill, M. R.; de Boer, B. G.; Mendak, S. J. *Inorg. Chem.* **1975**, *14*, 2041. (b) Churchill, M. R.; Kalra, K. L. *Inorg. Chem.* **1974**, *13*, 1899.
(19) van Koten, G.; Noltes, J. G. In *Comprehensive Organometallic Chemistry*; Wilkinson, G., Stone, F. G. A., Abel, E., Eds.; Pergamon: New York, 1982; Vol. 2, Chapter 14, pp 722−742.
(20) Hathaway, B. J. In *Comprehensive Coordination Chemistry*; Wilkinson, G., Gillard, R. J., McCleverty, J. A., Eds.; Pergamon: Oxford, U.K., 1987; Vol. 5, p 533.
(21) (a) Müller, A.; Schimanski, U. *Inorg. Chim. Acta* **1993**, *77*, L187. (b) Kang, H. C.; Do, Y.; Knobler, C. B.; Hawthorne, M. F. *Inorg. Chem.* **1988**, *27*, 1716. (c) Rao, C. P.; Dorfman, J. R.; Holm, R. H. *Inorg. Chem.* **1986**, *25*, 428. (d) Ho, D. M.; Bau, R. *Inorg. Chem.* **1983**, *22*, 4079. (e) Bresciani, N.; Marsich, N.; Nardin, G.; Randaccio, L. *Inorg. Chim. Acta* **1974**, *10*, L5. (f) Tiethof, J. A.; Stalick, J. K.; Corfield, P. W. R.; Meek, D. W. *J. Chem. Soc., Chem. Commun.* **1972**, 1141. (g) Chan, C.-K.; Guo, C.-X.; Wang, R.-J.; Mak, T. C. W.; Che, C.-M. *J. Chem. Soc., Dalton Trans.* **1995**, 753.
(22) Hubberstey, P.; Russell, C. E. *J. Chem. Soc., Chem. Commun.* **1995**, 959.
(23) (a) Messerschmidt, A.; Luecke, H.; Huber, R. *J. Mol. Biol.* **1993**, *230*, 997. (b) Messerschmidt, A.; Ladenstein, R.; Huber, R.; Bolognesi, M.; Avigliano, L.; Petruzelli, R.; Rossi, A.; Finazzo-Agró, A. *J. Mol. Biol.* **1992**, *224*, 179. (c) Zaitseva, I.; Zaitsev, V.; Card, G.; Moshkov, K.; Bax, B.; Ralph, A.; Lindley, P. *J. Biol. Inorg. Chem.* **1996**, *1*, 15. (d) Hiep-Hoa, N. T.; Nakagawa, K. H.; Hedman, B.; Elliott, S. J.; Lidstrom, M. E.; Hodgson, K. O.; Chan, S. I. *J. Am. Chem. Soc.* **1996**, *118*, 12766.
(24) (a) Karlin, K. D.; Gan, Q.-F.; Farooq, A.; Liu, S.; Zubieta, J. *Inorg. Chem.* **1990**, *29*, 2551. (b) Adams, H.; Bailey, N. A.; Dwyer, M. J. S.; Fenton, D. E.; Hellier, P. C.; Hempstead, P. D.; Latour, J.-M. *J. Chem. Soc., Dalton Trans.* **1993**, 1207.
(25) (a) Trofimenko, S. *Chem. Rev.* **1993**, *93*, 943.

accessible potential window. The CV of **2** is identical to that of **1**, confirming that the two complexes differ only in their oxidation states. We could also prepare **2** by chemical oxidation of **1** with the ferrocenium ion; the material prepared in this way was spectroscopically identical to that prepared earlier. The cathodic potential of the first process indicates that **1** has sufficient structural flexibility to permit the necessary distortion at the oxidized metal center to occur easily. Oxidation of a Cu(I) complex to the Cu(II) state generally results in a change in geometry from pseudotetrahedral in the Cu(I) state to a more nearly tetragonal geometry in the Cu(II) state [to satisfy the stereoelectronic preferences of the Cu(II) ion].[1,2,26] The potential at which this interconversion occurs is related to the ease with which the required geometric rearrangement can occur, and various sterically hindered complexes where conformational change of the coordination geometry is difficult require more positive potentials to attain the Cu(II) state than do unhindered complexes where the distortion is easier.[1,2] The geometric change is in part parameterised by the angle θ, the dihedral angle between the two CuN_2 planes, which is 90° for a pseudotetrahedral (D_{2d}) structure and 0° for a planar structure (D_{2h}). In practice, solid-state θ values tend to be around 70−80° for Cu(I) complexes,[1,2] which decreases to 40−50° for Cu(II) complexes depending on the steric properties of the ligands.[2,26]

Allosteric Properties. The 640 mV separation between the two couples is considerably larger than could be accounted for by a through-space Coulombic effect alone, and there are no direct bridging ligands to transmit an electronic interaction. The reason for the highly anodic potential of the second redox couple is therefore likely to be geometric: This redox potential is characteristic of Cu(I) complexes in which encapsulation of the metal prevents distortion away from tetrahedral geometry toward planarity.[1c,2] Successive oxidations of **1** therefore display negative cooperativity as a result of the structural changes that occur at each step, *i.e.* an allosteric effect.[27] The first oxidation triggers a structural change at that metal site which, when transmitted through the relatively rigid ligand array to the remaining metal sites, renders further structural distortion—and hence the second oxidation—more difficult. We found no evidence for a third Cu(I)/Cu(II) couple even at extreme positive potentials. Conversely, starting from the oxidized Cu^{I}/Cu^{II}_2 form, the first reduction induces a geometric change which relaxes the structure and so makes the second reduction easier: In this direction the cooperativity is positive.

Redox-induced structural changes have interesting possibilities in the design of complexes exhibiting cooperative behavior. Cooperativity is an important feature in multicomponent biological systems; a good example is hemoglobin,[28] where the binding of oxygen at one of the heme subunits causes a structural change which makes binding of a second molecule of oxygen, at an adjacent heme subunit, easier. This results in a "cascade" of successively easier binding of O_2 molecules at the heme sites. In reverse, dissociation of O_2 from one site results in a structural change which makes further dissociation easier, and so on. This type of long-distance control regulated by structural change is called the allosteric effect.[27] Some coordination complexes can, in a simple way, show the same effect.[27,29,30] Such complexes contain ligands with two or more binding sites linked in such a way that, for example, coordination of a metal at one site results in a structural change which increases (positive cooperativity) or decreases (negative cooperativity) the affinity of the second site for a metal ion.

In most of the artificial complexes which exhibit allosteric behavior, the necessary conformational change which triggers the effect arises from coordination of a metal ion. It is also in principle possible to exploit an electrochemically-induced conformational change, such as that shown by $[Cu(diimine)_2]^+$-type complexes. An example of this is given by the complex $[Cu_2(Me_4qp)_2]^{2+}$ [Me_4qp = 5,5′,3″,5‴-tetramethyl-2,2′:6′,2″:6″,2‴-quaterpyridine], which contains two $\{Cu(bipy)_2\}^+$-type fragments in a double helical structure.[31] Oxidation of one metal ion results in a structural change which is transmitted through the ligand system to the second site. It becomes more difficult for the second site also to change its geometry: the "slack" in the structure is largely taken up by the first oxidation. The potential of the second Cu(I)/Cu(II) couple is therefore 0.2 V more positive than the first, a separation which cannot be accounted for by simple electrostatic effects. We believe that **1** shows the same behavior but in a more extreme form because of the greater rigidity of the ligand framework.

Oxidation of all three metals would presumably result in decomposition to give a mononuclear Cu(II) complex of the type we have previously described,[15] which is obtained by direct reaction of the ligand with Cu(II) salts. The slow decomposition of the doubly-oxidized Cu^{I}/Cu^{II}_2 species is also likely to afford this product. There are other examples in the literature of polynuclear Cu(I) complexes which decompose to give mononuclear Cu(II) complexes on oxidation, as the only way of achieving the required tetragonal geometry.[31,32]

EPR Spectra of 2. The isotropic solution EPR spectrum of **2** is a poorly resolved quartet at room temperature, corresponding to hyperfine coupling to one Cu nucleus ($I = {}^3/_2$). The resolution improves somewhat with increasing temperature; the spectrum at 355 K is shown in Figure 4. The interpretation is straightforward and gives the parameters listed in Table 3.

Spectra of **2** recorded as frozen glasses exhibit a spectrum with seven resolved features (Figure 5a) which is independent of temperature between 77 and 120 K. The spectrum can be interpreted as approximately axial, with hyperfine coupling to a single nucleus giving two overlapping quartets with similar hyperfine splittings. However computer simulations based on this are in poor agreement with the observed spectrum, particularly in the low-field region where the amplitudes of the first four features increase in the approximate ratio 1:2:3:4, which is more consistent with the pattern expected from coupling to two equivalent Cu nuclei.[8−10] The series begun by the three low-field features should end approximately midway between the two highest-field features if the principal axes of

(26) (a) Gouge, E. M.; Geldard, J. F.; Sinn, E. *Inorg. Chem.* **1980**, *19*, 3356. (b) Foley, J.; Tyagi, S.; Hathaway, B. J. *J. Chem. Soc., Dalton Trans.* **1984**, 1. (c) Gouteron, J.; Jeannin, S.; Jeannin, Y.; Livage, J.; Sanchez, C. *Inorg. Chem.* **1984**, *23*, 3387. (d) Davis, W. M.; Zask, A.; Nakanishi, K.; Lippard, S. J. *Inorg. Chem.* **1985**, *24*, 3737. (e) Yokoi, H.; Addison, A. W. *Inorg. Chem.* **1977**, *16*, 1341.

(27) Lehn, J.-M. *Supramolecular Chemistry*, VCH: Weinheim, Germany, 1995.

(28) (a) Stryer, L. *Biochemistry*, 4th ed.; Freeman: New York, 1995. (b) Perutz, M. F. *Nature* **1970**, *228*, 726.

(29) (a) Rebek, J. R. *Acc. Chem. Res.* **1984**, *17*, 258. (b) Beer, P. D. *Chem. Soc. Rev.* **1989**, *18*, 409.

(30) A representative recent selection of artificial molecules displaying allosteric behavior: (a) Rodriguez-Ubis, J. C.; Juanes, O.; Brunet, E. *Tetrahedron Lett.* **1994**, *35*, 1295. (b) Gagnaire, G.; Jeunet, A.; Pierre, J.-L. *Tetrahedron Lett.* **1991**, *32*, 2021. (c) Toupance, T.; Ahsen, V.; Simon, J. *J. Am. Chem. Soc.* **1994**, *116*, 5352. (d) Rissanen, K.; Breitenbach, J.; Huuskonen, J. *J. Chem. Soc., Chem. Commun.* **1994**, 1265. (e) Schneider, H.-J; Werner, F. *J. Chem. Soc., Chem. Commun.* **1992**, 490. (f) Baldes, R.; Schneider, H.-J. *Angew. Chem., Int. Ed. Engl.* **1995**, *34*, 321.

(31) Gisselbrecht, J.-P.; Gross, M.; Lehn, J.-M.; Sauvage, J.-P.; Ziessel, R.; Piccini-Leopardi, C.; Arrieta, J. M.; Germain, G.; Van Meersche, M. *Nouv. J. Chim.* **1984**, *8*, 659.

(32) Yao, Y.; Perkovic, M. W.; Rillema, D. P.; Woods, C. *Inorg. Chem.* **1992**, *31*, 3956.

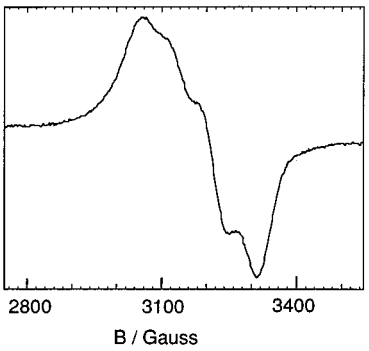

Figure 4. X-band EPR spectrum of **2** in 1,2-dichloroethane/thf (1:1) at 355 K.

Table 3. EPR Parameters for **2**[a]

(a) Isotropic Parameters[b]

$\langle g \rangle$	$\langle A^{Cu} \rangle$
2.1183	73.6

(b) Anisotropic Parameters

T/K	g_x	g_y	g_z	A_x	A_y	A_z
120	2.086(5)	2.128(5)	2.206(1)	40(10)[c]	40(10)[c]	105(1)[c]
160	2.062(5)	2.062(5)	2.254(5)	35[d]	35[d]	150(5)[d]

[a] Hyperfine couplings in units of 10^{-4} cm^{-1}. [b] At 355 K. [c] Coupling to two equivalent Cu nuclei with *x* and *y* axes displaced ±16° from the corresponding *g*-matrix axes. [d] Coupling to one Cu nucleus.

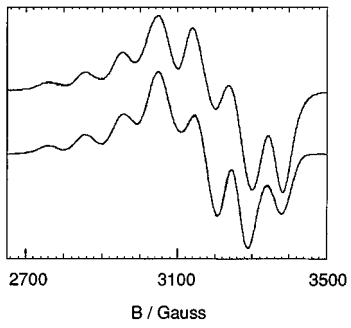

Figure 5. X-band EPR spectrum of **2** in 1,2-dichloroethane/thf (1:1) at 120 K: Top, experimental spectrum; bottom, computer simulation using the parameters of Table 3 and Gaussian widths of 25 G.

the *g* and the two hyperfine matrices are coincident. If, in fact, the feature at highest field is to be accounted for, it is not possible to have coincident axes. Least-squares fitting of the three low-field features and the feature at highest field, assuming that the *x*- and *z*- hyperfine axes are displaced by an angle $\pm\beta$ from the corresponding *g*-matrix axes, yields g_x, g_z, A_z, and the angle β; the fit is insensitive to A_x. Computer simulations allow estimation of A_x, along with g_y and A_y, albeit with considerable margins of error. The best-fit parameters are summarized in Table 3, and Figure 5 also shows the computer simulation based on these parameters.

As the temperature is increased above 120 K, the features of the well-resolved 120 K spectrum first broaden and then disappear until, at 160 K, a very different spectrum (Figure 6) is obtained. This spectrum is approximately axial with hyperfine coupling to a single Cu nucleus; approximate values of $A_{||}$, $g_{||}$ and $g_\perp$, can be measured from the spectrum (Table 3). The *g*-matrix components are in reasonable agreement with the isotropic *g*-value, $\langle g \rangle = 2.126$. A simulation with $A_\perp = (3\langle A \rangle - A_{||})/2$, also shown in Figure 6, is in reasonable agreement with the experimental spectrum.

Interpretation of EPR Parameters. Assuming that, in the high-temperature limiting structure, the singly-occupied molecular orbital (SOMO) is predominantly a single Cu d($x^2 - y^2$) orbital (eq 1), the predicted hyperfine matrix components

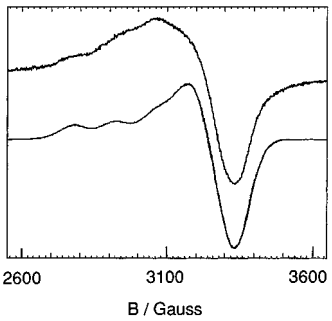

Figure 6. X-band EPR spectrum of **2** in 1,2-dichloroethane/thf (1:1) at 160 K: Top, experimental spectrum; bottom, computer simulation using the parameters of Table 3 and Gaussian widths of 50 G.

$$|\mathrm{SOMO}\rangle = c|x^2 - y^2\rangle + ... \quad (1)$$

$$A_x = A_s + P(2/7\rho^d + \Delta g_x - 3/14\Delta g_y) \quad (2a)$$

$$A_y = A_s + P(2/7\rho^d + \Delta g_y - 3/14\Delta g_x) \quad (2b)$$

$$A_z = A_s + P[-4/7\rho^d + \Delta g_z + 3/14(\Delta g_x + \Delta g_y)] \quad (2c)$$

are given by eqs 2,[33] where A_s is the isotropic contribution of the s-orbital spin density, ρ^d ($=c^2$) is the d-electron spin density, $\Delta g_i = g_i - g_e$, and P ($=408 \times 10^{-4}$ cm^{-1})[34] is the dipolar coupling parameter for Cu. Assuming that $A_{||}$, $A_\perp$, and $\langle A \rangle$ are all negative, eq 3 leads to $\rho^d = 0.60$ for the high-temperature

$$A_z - \langle A \rangle = P[-4/7\rho^d + 2/3\Delta g_z - 5/42(\Delta g_x + \Delta g_y)] \quad (3)$$

spectrum. This value is significantly smaller than that normally obtained for those copper complexes which have a basically square planar geometry, where the magnetic orbital is essentially pure d($x^2 - y^2$).[35]

Equation 3 can be used to analyze the parameters from the low-temperature (77−120 K) delocalized spectrum if we neglect the nonconcidence of the principal axes. Assuming that A_x, A_y, and A_z are all negative, we obtain $\rho^d = 0.38 \pm 0.03$, where the uncertainty reflects the very approximate values of A_x and A_y. Spin−orbit coupling corrections to the SOMO wave function lead to extra terms in the matrix elements of both the electronic Zeeman and hyperfine Hamiltonians which involve the average energy differences between d($x^2 - y^2$) and d(*xy*), d(*xz*), and d(*yz*). These corrections apply to both the *g*- and *A*-matrices, and when the principal axes are coincident, the *A*-matrix corrections can be expressed in terms of the *g*-anisotropies, as in eqs 2 and 3. When the matrix principal axes are noncoincident, the *g*- and *A*-correction terms differ by factors of the order of $\cos^2 \beta$. With $\beta \approx 16°$, the use of eq 3 without modification thus introduces an error of *ca.* 8%, comparable to the experimental uncertainty already accounted for.

The EPR parameters for the low-temperature delocalized form of **2** therefore indicate that the principal axes corresponding to A_{max} are displaced from the g_{max} axis by ±16°. Assuming that the metal contributions to the SOMO are primarily d(x^2-y^2),

(33) Atherton, N. M. *Electron Spin Resonance*; Ellis Horwood: Chichester, U.K., 1973; p 242.
(34) Morton, J. R.; Preston, K. F. *J. Magn. Reson.* **1978**, *30*, 577.
(35) (a) Hathaway, B. J. In *Comprehensive Coordination Chemistry*; Wilkinson, G., Gillard, R. D., McCleverty, J. A., Eds.; Pergamon: Oxford, U.K., 1987; Vol. 5, pp 662−673. (b) Bertini, I.; Gatteschi, D.; Scozzafava, A. *Coord. Chem. Rev.* **1979**, *29*, 67.

this means that the two approximate mean coordination planes are side-by-side but with their normals tilted by ±16° from the internuclear vector. This is very similar to the arrangement of the more closely-spaced pair Cu(2) and Cu(3) in the crystal structure of **1** (Figure 1b). Presumably Cu(1) remains more distant and is not involved in the delocalization mechanism. This is related to the structures of the tricopper site of multicopper oxidases, which contain a pair of interacting Cu centers (a type 3 site) with a more remote isolated type 1 Cu site.[5,23] As the temperature is increased above 120 K, the delocalization pathway is apparently disrupted, and at 160 K, the unpaired electron is localized (on the EPR time scale) on one Cu center. This is also consistent with the NMR results for **1** where, in solution at room temperature, the distortion present in the crystal which results in two metal ions being close together is removed. The geometry implied by the EPR parameters is consistent with the presence of the π-stacking interaction between ligand aromatic rings associated with these Cu atoms that was observed in the crystal structure of **1** (Figure 1b). It is plausible that this π-stacking provides a spin delocalization pathway, and we note that we[12] and others[36] have previously shown that magnetic exchange interactions can be propagated *via* aromatic π-stacking in the absence of direct bridges between the interacting metal centers. This is the first time that such a delocalisation pathway has been observed in mixed-valence copper complexes; all of the other examples involve either very short metal−metal separations (<2.5 Å) with direct overlap of metal d-orbitals[8] or a bridging atom such as phenolate or thiolate between the two metal centers.[9,10] The temperature-dependent behavior of **2** is in interesting contrast to the more common situation where the unpaired electron of a Cu(I)/Cu(II) pair is localized at low temperatures but becomes delocalized as the temperature increases.[9d]

In the absence of a crystal structure for **2**, the parameters from the 160 K spectrum give some useful information on the geometry of the now valence-localized Cu(II) center. The EPR spectra of $Cu^{II}(NN)_2$ complexes are sensitive to the angle θ between the two CuNN planes, and this provides a useful indication of the geometry.[37−39] Specifically, in pseudotetrahedral ($\theta = 90°$; D_{2d}) geometries the value of $g_{||}$ is high (>2.3) and the value of $A_{||}$ is low. As the geometry changes toward planar ($\theta = 0°$; D_{2h}) the value of $g_{||}$ decreases and that of $A_{||}$ increases. For example, a near-tetrahedral $Cu(pz_2)_2$ (pz = pyrazolyl) complex with $\theta = 71.9°$ has $g_{||} = 2.316$, $g_{\perp} = 2.041$, $A_{||} = 95 \times 10^{-4}$ cm^{-1}, and $A_{\perp} = 50 \times 10^{-4}$ cm^{-1}. The same donor set in a planar geometry gives $g_{||} = 2.209$, $g_{\perp} = 2.031$, $A_{||} = 206 \times 10^{-4}$ cm^{-1}, and $A_{\perp} = 34 \times 10^{-4}$ cm^{-1}.[37] There are several other examples of this behavior.[38,39]

The EPR parameters for **2** at 160 K (Table 3) are entirely consistent with a geometry for the Cu(II) center roughly midway between planar and pseudotetrahedral with a $d(x^2 - y^2)$ ground state. The complex $[Cu(Tp^{Py})(H_2O)][PF_6]$, which has a planar N_4 donor set from two arms of $[Tp^{Py}]^-$ and an elongated axial water ligand, serves as a useful comparison for the planar extreme with this donor set: It has $g_{||} = 2.238$, $g_{\perp} = 2.073$, and $A_{||} = 196 \times 10^{-4}$ cm^{-1}.[15] The substantially lower value of $A_{||}$ for **2** (150×10^{-4} cm^{-1}) and the slightly higher value of $g_{||}$ (2.254) are consistent with the expected distortion away from planarity for the Cu(II) center of **2**. The *g*-values of **2** are almost identical to those for the powder EPR spectrum of $[Cu(bipy)_2]^{2+}$,[39] which has a geometry exactly midway between planar and pseudotetrahedral ($\theta = 44.6°$), and the parameters (especially $A_{||}$) are also in reasonable agreement with another $Cu^{II}(NN)_2$ complex with a θ values of 61.3°.[38a] Given that the values of θ for the three Cu(I) centers of **1** are all above 80°, this suggests that a reasonable amount of structural reorganization can occur when **1** is oxidized to **2**, but (following the discussion of the electrochemical data above) this cannot occur a second time. Of course the parameter θ alone is an oversimplistic way of characterizing irregular four-coordinate geometries,[3] but in the absence of a crystal structure for **2** the level of analysis given above is all that is justified.

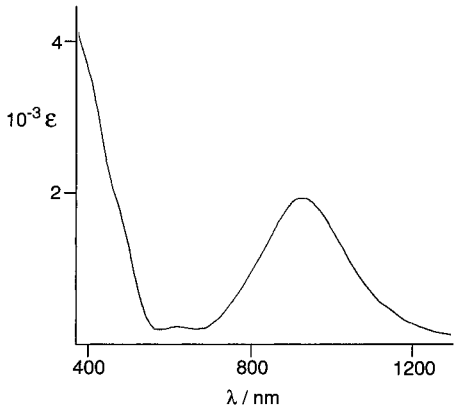

Figure 7. Part of the electronic spectrum of **2** in CH_2Cl_2.

Electronic Spectra. The electronic spectrum of **1** in MeCN solution shows the expected ligand-based $\pi-\pi^*$ transitions at wavelengths below 300 nm and Cu(I)-to-ligand MLCT bands[1−5] at longer wavelengths (see Experimental Section); these are all as expected and unremarkable.

The electronic spectrum of **2** in MeCN solution shows a strong, broad transition at 910 nm (ϵ 2100 dm^3 mol^{-1} cm^{-1}), with a width at half-maximum height of 3400 cm^{-1} (Figure 7). In addition there are the expected ligand-centered transitions in the UV region. The position and intensity of the 910 nm band are not significantly solvent dependent across a range of solvents including CH_2Cl_2, DMSO, and aqueous acetone (1:4). This transition disappears when the complex in solution is reduced by addition of ascorbic acid; conversely, solutions of **1** when exposed to the air for prolonged periods slowly develop this transition. It is therefore associated with the presence of a Cu(II) center in the complex.

There are two possible assigments for this band: one or more metal-centered d−d transitions or an intervalence charge-transfer (IVCT) band (or possibly a superposition of both). In Cu(II) complexes with tetrahedrally-distorted N_4 coordination environments, the d−d transitions move to low energy and gain in intensity compared to those of planar complexes.[38a,40] Transitions in the region of 800−1000 nm are indicative of Cu(II) in pseudotetrahedral environments. The extinction coefficients of such transitions are generally a few hundred dm^3 mol^{-1} cm^{-1}, although they can very occasionally be as high as *ca.* 1000 dm^3 mol^{-1} cm^{-1}. The extinction coefficient value of 2100 dm^3 mol^{-1} cm^{-1} for the 910 nm transition in **2** is therefore higher than any other examples we are aware of, and for this reason

(36) Brondino, C. D.; Calvo, R.; Atria, A. M.; Spodine, E.; Peña, O. *Inorg. Chim. Acta* **1995**, *228*, 261.
(37) (a) Herring, F. G.; Patmore, D. J.; Storr, A. *J. Chem. Soc., Dalton Trans.* **1975**, 711. (b) Patmore, D. J.; Rendle, D. F.; Storr, A.; Trotter, J. *J. Chem. Soc., Dalton Trans.* **1975**, 718.
(38) (a) Davis, W. M.; Zask, A.; Nakanishi, K.; Lippard, S. J. *Inorg. Chem.* **1985**, *24*, 3737. (b) Knapp, S.; Keenan, T. P.; Zhang, X.; Fikar, R.; Potenza, J. A.; Schugar, H. J. *J. Am. Chem. Soc.* **1990**, *112*, 3452. (c) Attanasio, D.; Tomlinson, A. A. G.; Alagna, L. *J. Chem. Soc., Chem. Commun.* **1977**, 618. (d) Dudley, R. J.; Hathaway, B. J.; Hodgson, P. G. *J. Chem. Soc., Dalton Trans.* **1972**, 882.
(39) Foley, J.; Tyagi, S.; Hathaway, B. J. *J. Chem. Soc., Dalton Trans.* **1984**, 1.
(40) (a) Gouge, E. M.; Geldard, J. F. *Inorg. Chem.* **1978**, *17*, 270. (b) Yokoi, H.; Addison, A. W. *Inorg. Chem.* **1977**, *16*, 1341.

we think that it is unlikely to arise solely from a d−d transition, especially as $[Cu(bipy)_2]^{2+}$ (whose EPR parameters are in very close agreement with **2**, indicating a similar geometry) has a maximum at 665 nm in its solid-state reflectance spectrum (extinction coefficient not given).[39]

Intervalence charge-transfer bands in mixed-valence Cu(I)/Cu(II) complexes generally occur in the near-IR region of the electronic spectrum and have extinction coefficients of several hundred or a few thousand $dm^3\ mol^{-1}\ cm^{-1}$,[8,9] so both the position and intensity of the 910 nm peak are consistent with it being an IVCT. The EPR spectrum of **2** under these conditions shows that it is valence trapped, *i.e.* class I or class II according to the Robin and Day classification;[41] if it were class III (fully delocalized) then a 7-line EPR spectrum would have been observed.[8−10] For the transition to be an IVCT band therefore requires **2** to be class II under these conditions, because localized class I complexes do not show IVCT behavior. A d−d transition would also be expected in addition to the IVCT, but since this could be an order of magnitude weaker and in a similar position to the IVCT band, it could easily be obscured.

IVCT transitions in class II mixed-valence complexes can be analyzed by eq 4 deriving from Hush theory.[42] V_{ab} (the

$$V_{ab} = (0.0205/r)(\epsilon_{max}\Delta\tilde{\nu}_{1/2}\tilde{\nu}_{op})^{1/2} \quad (4)$$

electronic coupling matrix element), $\Delta\tilde{\nu}_{1/2}$ (the half-width of the band), and $\tilde{\nu}_{op}$ (the optical band maximum) are in cm^{-1}, ϵ_{max} is the extinction coefficient of the band in $dm^3\ mol^{-1}\ cm^{-1}$, and r is the metal−metal separation in Å (estimated as 3.3 Å from the average of the metal−metal separations in **1**).

Application of this to the 910 nm transition (assuming that it is an IVCT transition and the d−d transition under it is negligibly small in comparison) gives $V_{ab} \approx 1700\ cm^{-1}$, which is an upper limit since some of the band intensity is likely to be from a d−d transition. Values of V_{ab} of *ca.* $1000\ cm^{-1}$ occur in strongly-interacting class II Ru(II)/Ru(III) mixed-valence systems;[43] the Creutz−Taube ion, generally considered to be on the class II/class III borderline, has $V_{ab} > 3000\ cm^{-1}$.[44,45] Detailed interpretation of the data for **2** is not justified because of the possible contribution of the d−d transition to the bandwidth and intensity and possible asymmetry in the metal sites which has not been allowed for; however this does suggest that the complex is at the more strongly interacting end of class II behavior (valence-trapped but a significant metal−metal interaction), in agreement with the EPR results.

The absence of solvatochromism for the IVCT transition could arise because the constrained and relatively rigid ligand framework prevents structural reorganization following the charge transfer. While solvatochromism does indicate class II behavior, the converse is not necessarily true: There are other examples of class II mixed-valence complexes whose IVCT bands are not significantly solvatochromic.[45]

Conclusions

The structure of $[Cu_3(Tp^{Py})_2][PF_6]$ (**1**) arises from the requirement of each Cu(I) ion to be four-coordinate and the spread-out disposition of the bidentate chelating arms of the podand ligand; it may be contrasted with the tetramers $[M_4(Tp^{Py})_4][PF_6]_4$ that arise with dications such as Mn(II) which prefer six coordination. The isosceles triangular array of Cu(I) centers with N-donors is structurally reminiscent of the tris-Cu(I) site of ascorbate oxidase. The electrochemical behavior shows that whereas one Cu(I)/Cu(II) oxidation is relatively facile and results in a degree of rearrangement of the geometry about the metal center which is oxidized, a second oxidation is much more difficult ($\Delta E_{1/2} = 640$ mV) as further rearrangement is not possible; this is an example of an allosteric effect, whereby a structural change at one site effects the properties of another site. The mixed-valence $Cu^{I}_2Cu^{II}$ complex **2** shows delocalization of the unpaired electron between *two* metal centers below 120 K; above 160 K the unpaired electron is localized, possibly because increased thermal motion disrupts the π-stacking pathway which facilitates delocalization at low-temperatures. The electronic spectrum of **2** in fluid solution shows an intense transition in the near-IR region which we believe to be an IVCT band.

Acknowledgment. We thank the EPSRC for grants to purchase the EPR spectrometer and the SMART diffractometer and Unilever Research for financial support (P.L.J.).

Supporting Information Available: Tables of X-ray experimental details and crystallographic data, all atomic coordinates, anisotropic thermal parameters, and bond distances and angles for the crystal structure of **1**·$(MeCN)_2$ (11 pages). Ordering information is given on any current masthead page.

IC970088Q

(41) Robin, M. B.; Day, P. *Adv. Inorg. Chem. Radiochem.* **1967**, *10*, 247.
(42) (a) Hush, N. S. *Prog. Inorg. Chem.* **1967**, *8*, 391. (b) Creutz, C. *Prog. Inorg. Chem.* **1983**, *30*, 1. (c) Hush, N. S. *Coord. Chem. Rev.* **1985**, *64*, 135.
(43) Ward, M. D. *Chem. Soc. Rev.* **1995**, *24*, 121.
(44) Bardwell, D. A.; Horsburgh, L.; Jeffery, J. C.; Joulié, L. F.; Ward, M. D.; Webster, I.; Yellowlees, L. J. *J. Chem. Soc., Dalton Trans.* **1996**, 2527.
(45) Richardson, D. E.; Taube, H. *Coord. Chem. Rev.* **1984**, *60*, 107.